

Modified muffin-tin potential for the study of semiconductors using the orthogonalized-plane-wave method

Michihide Kitamura

Department of Electrical and Electronic Engineering, Utsunomiya University, Utsunomiya 321, Japan

(Received 22 June 1994; revised manuscript received 29 August 1994)

The positions of empty lattices (EL's) are defined as the positions obtained by shifting the real lattices by $a_0/2$ along the [100] direction and, in order to study how the crystal potentials of semiconductors with small packing fraction should be represented within the framework of a muffin-tin (MT) approximation, the MT potentials are constructed on the EL sites. Furthermore, in order to take into account the effect of a nonspherical potential due to the site symmetry of T_d , the nonspherical potential whose angular momentum $l=3$ is built up. The electronic structures of the common semiconductors Si, Ge, GaAs, ZnSe, InSb, and CdTe are calculated by a method in which the nonspherical potential and the MT potential on the EL site are introduced into the orthogonalized-plane-wave method within the framework of the MT approximation based on the self-consistent-field atomic-structure calculations. It is shown that the symmetry of the potential consisting of MT potentials on real atoms and EL sites coincides with that of the nonspherical potential, which is closely related to sp^3 hybrid orbitals, and that the calculations including both the nonspherical potentials and the MT potentials on the EL sites predict fairly well the experimental facts rather than the calculations using only the MT potentials on the real atoms.

I. INTRODUCTION

There are many different kinds of electronic structure calculations of condensed matter,^{1,2} which differ in how the potential is constructed and what mathematical expansion of the wave function is used. However, all calculations should give reasonable answers if the appropriate potential is used and if the expansion is complete enough. Actually, I studied the electronic structures of perovskite-type compounds³ and a K_2PdCl_6 crystal⁴ and the elastic properties of semiconductors^{5,6} by the extended Hückel tight-binding (XHTB) (Refs. 3, 4, and 6) and universal tight-binding parameters (UTBP) (Ref. 5) methods, and obtained results which are consistent with the corresponding experiments. On the other hand, recently I calculated the electronic structures of rare-earth hexaborides RB_6 with no adjustable parameters using a modified orthogonalized-plane-wave (MOPW) method within the framework of the muffin-tin (MT) approximation based on self-consistent-field (SCF) atomic-structure calculations,⁷ and also found results which are reasonable for a comparison with experiments. In the MOPW method, the wave function is expanded by the linear combination of the wave functions of the orthogonalized-plane-wave (OPW) and tight-binding (TB) methods, so I think that the MOPW method is also applicable to the study of the electronic structures of magnetic semiconductors (MS's) like $Cd_{1-x}Mn_xTe$ in which the $3d$ orbits of Mn atoms form the TB basis sets in the MOPW method. In the present paper, before proceeding to the study of MS's by the MOPW method, we consider as a first step how the electronic structures of zinc-blende-structure semiconductors (ZBS's) which are the host crystals of MS's, are calculated by the OPW method within the framework of the MT approximation based on the

SCF calculations, because for the study of the valence- and conduction-band structures of the common semiconductors it is not necessary to take into account the effect of the localized d or f orbits such as the $3d$ orbits of Mn atoms.

In the present paper, the well-known OPW method based on the MT approximation is adopted for the study of the ZBS's, so the reader may think that there is no additional finding to be mentioned. However, it is well known that the MT approximation does not work well for crystals with a small packing fraction. Actually, the packing fraction of the ZBS's is small, e.g., that of rare-earth hexaborides is 74.7%, but that of Si is 34%, so the electronic structures of the ZBS's have usually been calculated by using the TB method⁸ or pseudopotential method⁹ instead of the method based on the MT approximation. One of the aims of this paper, therefore, is to show how the crystal potential of a crystal with a small packing fraction should be represented within the framework of the MT approximation. In addition to this fact of small packing fraction, furthermore, ZBS's form sp^3 hybrid orbitals as a reflection of the effect of the nonspherical potential. Therefore, in the study of ZBS's, the effect of the nonspherical potential must be taken into account as accurately as possible even in the method based on the MT approximation. In many calculations within the framework of a scattering mechanism based on the MT approximation, e.g., the band-structure calculation based on a linearized-augmented-plane-wave (LAPW) method of a magnetic semiconductor $Cd_{1-x}Mn_xTe$ carried out by Wei and Zunger,¹⁰ the most essential quantity is the phase shift for an electron scattering by the MT potential. I have also calculated the x-ray-absorption near-edge structures (XANES) of some crystals using a multiple-scattering (MS) theory based on the MT approx-

imation.^{4,11,12} Usually the phase shift is calculated for only the spherical potential, so if we wish to study the electronic structure of matter in which the effect of the nonspherical potential cannot be neglected, we have to solve the scattering problem for the nonspherical potential. This is not so easy a problem. In the OPW method, however, since the effect of the crystal potential is evaluated by an integrated form such as a Fourier component of the crystal potential, once the nonspherical potential is built up the effect of the nonspherical potential can easily be evaluated as compared with the methods based on the scattering mechanism like APW or Korringa-Kohn-Rostoker (KKR). This is the reason why, in the present paper, the OPW method based on the MT approximation is adopted for the study of electronic structures of the ZBS's whose packing fraction is small and in which the effect of the nonspherical potential cannot be neglected. The second purpose of this paper is to do the calculation taking into account the effect of the nonspherical potential as correctly as possible and to compare the calculated results with the experiments or other calculations. Let us remember that a calculation should give a reasonable answer if the appropriate potential is used and if the

mathematical expansion of the wave function is complete enough.

The aim of this paper is to show how the electronic structures of zinc-blende-structure semiconductors (ZBS's) are calculated by a method based on the MT approximation. Since the effect of the nonspherical potential cannot be neglected in ZBS's, the nonspherical potential due to the site symmetry of T_d is constructed, and the Fourier components for the nonspherical potential are added into those for the MT potential. Moreover, in order to increase the packing fraction, the MT potential on an empty lattice (EL) site is introduced into the OPW method within the framework of the MT approximation based on the SCF atomic-structure calculations.

II. THEORY

A. Crystal potential

The crystal potential $V_{\text{cry}}(\mathbf{r})$ consists of the spherical $V_{\text{cry}}^{(s)}(r)$ and nonspherical $V_{\text{cry}}^{(\text{ns})}(\mathbf{r})$ terms, and is given as follows:¹¹

$$V_{\text{cry}}(\mathbf{r}) = V_{\text{cry}}^{(s)}(r) + V_{\text{cry}}^{(\text{ns})}(\mathbf{r}), \quad (1a)$$

$$V_{\text{cry}}^{(s)}(r) = V_c^{(s)}(r) - 6\alpha_{\text{ex}}(3\rho^{(s)}(r)/8\pi)^{1/3}, \quad (1b)$$

$$V_{\text{cry}}^{(\text{ns})}(\mathbf{r}) = V_c^{(\text{ns})}(\mathbf{r}) - 6\alpha_{\text{ex}}(3/8\pi)^{1/3}[\{\rho^{(s)}(r) + \rho^{(\text{ns})}(\mathbf{r})\}^{1/3} - \rho^{(s)}(r)^{1/3}]. \quad (1c)$$

Usually, since the ratio $\rho^{(\text{ns})}(\mathbf{r})/\rho^{(s)}(r)$ of the spherical and nonspherical electron densities can be regarded as a small, Eq. (1c) is further approximated as follows:

$$V_{\text{cry}}^{(\text{ns})}(\mathbf{r}) = V_c^{(\text{ns})}(\mathbf{r}) - 2\alpha_{\text{ex}}(3/8\pi)^{1/3}\rho^{(s)}(r)^{-2/3}\rho^{(\text{ns})}(\mathbf{r}). \quad (1d)$$

The spherical term $V_{\text{cry}}^{(s)}(r)$ of the $V_{\text{cry}}(\mathbf{r})$ can be written in more explicit form by using the $V_c^{(s)}(r)$ and $\rho^{(s)}(r)$ evaluated as follows:

$$V_c^{(s)}(r) = V_c^{\text{at}}(r) + (2r)^{-1} \sum_{\alpha \neq 0} R_{\alpha}^{-1} \int_{R_{\alpha}-r}^{R_{\alpha}+r} r_{\alpha} W(r_{\alpha}) dr_{\alpha} + \sum_{\alpha \neq 0} 2\delta q_{\alpha}/R_{\alpha}, \quad (2a)$$

$$\rho^{(s)}(r) = \rho^{\text{at}}(r) + (2r)^{-1} \sum_{\alpha \neq 0} R_{\alpha}^{-1} \int_{R_{\alpha}-r}^{R_{\alpha}+r} r_{\alpha} \rho^{\text{at}}(r_{\alpha}) dr_{\alpha}, \quad (2b)$$

where a function $W(r_{\alpha})$ is the short-range function introduced in order to separate the long-range Coulombic part due to the charge transfer (whose value is given by δq_{α}) from the atomic Coulomb potential $V_c^{\text{at}}(r_{\alpha})$, and is defined as

$$W(r_{\alpha}) = V_c^{\text{at}}(r_{\alpha}) - 2\delta q_{\alpha}/r_{\alpha}. \quad (2c)$$

By using the spherical term $V_{\text{cry}}^{(s)}(r)$ of the crystal potential $V_{\text{cry}}(\mathbf{r})$, the MT potential characterized by the MT radius and the MT zero is constructed. From the physical point of view, the MT radius should be decided from the point in which crystal potentials calculated for

two different atoms separated by the minimum interatomic distance cross, and the MT zero should be given by the value obtained by averaging the crystal potentials over the whole volume except for the MT spheres region,¹¹ however, it is well known that in the ordinary calculations based on the MT approximation, if the MT zero obtained from the above scheme is used on the electronic structure calculations of matters, the bands subsequently found do not agree with the experimental facts, and that this discrepancy can be resolved by varying the magnitude of the MT zero until the agreement with the experiment is obtained.^{13,14} We will see in Sec. III that an averaged value of the MT potentials on the empty lattice sites corresponds to this energy variation for the MT zero.

B. Fourier components of the nonspherical potential

From Eq. (1d), the nonspherical potential $V_{\text{cry}}^{(\text{ns})}(\mathbf{r})$ is written as

$$V_{\text{cry}}^{(\text{ns})}(\mathbf{r}) = \sum_{\alpha \neq 0} \sum_{l \neq 0} \sum_m u_L(r_\alpha, r) Y_L(\hat{\mathbf{r}}), \quad (3a)$$

$$u_L(r_\alpha, r) = v_L(r_\alpha, r) - 2\alpha_{\text{ex}}(3/8\pi)^{1/3} \rho^{(s)}(r)^{-2/3} g_L(r_\alpha, r). \quad (3b)$$

Here, since $v_L(r_\alpha, r)$ and $g_L(r_\alpha, r)$ are defined by $\int d\hat{\mathbf{r}} Y_L^*(\hat{\mathbf{r}}) V_c^{\text{at}}(r_\alpha)$ and $\int d\hat{\mathbf{r}} Y_L^*(\hat{\mathbf{r}}) \rho^{\text{at}}(r_\alpha)$, respectively,¹¹ Eq. (3b) is further evaluated as

$$u_L(r_\alpha, r) = \int d\hat{\mathbf{r}} Y_L^*(\hat{\mathbf{r}}) h(r_\alpha, r), \quad (3c)$$

$$h(r_\alpha, r) = V_c^{\text{at}}(r_\alpha) - 2\alpha_{\text{ex}}(3/8\pi)^{1/3} \rho^{(s)}(r)^{-2/3} \rho^{\text{at}}(r_\alpha), \quad (3d)$$

where

$$V_c^{\text{at}}(r_\alpha) = -2Z_\alpha/r_\alpha + U(r_\alpha), \quad (3e)$$

$$\nabla^2 U(r_\alpha) = -8\pi \rho^{\text{at}}(r_\alpha). \quad (3f)$$

Here, in order to represent the coefficient $u_L(r_\alpha, r)$ given by Eq. (3c) as an analytical form, if we assume that the potential $h(r_\alpha, r)$ is given by $-2Z_\alpha^*/r_\alpha$ with a constant value Z_α^* , the coefficient $u_L(r_\alpha, r)$ can be evaluated as follows:

$$u_L(r_\alpha, r) = (-8\pi Z_\alpha^*/2l+1)(r^l/R_\alpha^{l+1}) Y_L^*(\hat{\mathbf{R}}_\alpha). \quad (4)$$

It is noted here that the constant value Z_α^* should be smaller than the atomic number Z_α because of the existing repulsive electron-electron interaction $U(r_\alpha)$ which satisfies the Poisson equation defined by Eq. (3f). By the way, group theory tells us that the maximum angular momentum l_{max} of the nonspherical potential for a site symmetry of T_d is 3, so if we focus our attention on only the largest nonspherical potential and the first-nearest-neighbor (FNN) atoms whose distance is d_0 , the nonspherical potential $V_{\text{cry}}^{(\text{ns})}(\mathbf{r})$ can be represented by the third order of cubic harmonics:

$$V_{\text{cry}}^{(\text{ns})}(\mathbf{r}) = (-40Z_{\text{FNN}}^*/\sqrt{3}d_0^4)xyz. \quad (5)$$

Here it should be mentioned that if the nonspherical potential of a cation is given by a form of Eq. (5), i.e., $-xyz$, that of an anion is given by the form of xyz , and furthermore it is instructive to note that the symmetry of the nonspherical potential, xyz , is closely related to the fact that sp^3 hybrid orbitals form an asymmetric electron density which is large for the $[111]$, $[1\bar{1}\bar{1}]$, $[\bar{1}1\bar{1}]$, and $[\bar{1}\bar{1}1]$ orientations and small for the $[\bar{1}\bar{1}\bar{1}]$, $[\bar{1}11]$, $[1\bar{1}1]$, and $[11\bar{1}]$ ones.

Fourier components $\langle \mathbf{G}' | V_{\text{cry}}^{(\text{ns})}(\mathbf{r}) | \mathbf{G} \rangle$ for the nonspherical potential given by Eq. (5), therefore, are evaluated as follows:

$$\langle \mathbf{G}' | V_{\text{cry}}^{(\text{ns})}(\mathbf{r}) | \mathbf{G} \rangle = \sum_{\mu} (N_{\mu}/V) e^{i\mathbf{q}\cdot\mathbf{d}_{\mu}} (-4\pi i) (-40Z_{\text{FNN}}^*/\sqrt{3}d_0^4) (q_x q_y q_z / q^3) \int_0^{R_{\text{MT}}^{(\mu)}} r^5 j_3(qr) dr, \quad (6)$$

where the meaning of symbols \mathbf{q} , \mathbf{d}_{μ} , N_{μ} and V is the same as in Ref. 7.

In the practical calculations of the band structures, we use the value of Z_{FNN}^* as a parameter which is adjusted so that the calculated result coincides with the experiment or other calculations.

C. MT potential on the empty lattice site

We define the positions of the empty lattices (EL's) as the positions obtained by shifting the real lattices by $a_0/2$ along the $[100]$ direction, where a_0 is the lattice constant. The unit cell consisting of both the real and empty lattices is shown in Fig. 1. This unit cell consists of eight small cubes, and each cube forms a bcc structure. The MT potentials on the EL sites, hereafter denoted as EL-MT potentials, are first principally calculated by the same method as described in Sec. II A with no difficulties. This point will be discussed below. There are two kinds of EL's: One is located on the position originating from the shift of a cation, and the other on the position originating from that of an anion. Therefore, the MT radius for the EL-MT potential of the former is given by that of the cation, and that of the latter is given by the MT radius of the anion. It is easily understood that by introducing the

EL's, the packing fraction becomes about 68%, which is two times larger than that of the ZBS's constituted from only the real lattices.

We have found that the packing fraction is increased by introducing the EL's. However, the most essential point to be mentioned in introducing the EL is that the EL-MT potential, whose origin of energy is of course the MT zero, is repulsive, contrary to that for the real atom. This is understood as follows: The EL can be regarded as an atom with atomic number $Z=0$ (hereafter we call it an empty atom), so the atomic potential of the empty atom is zero. Roughly speaking, the crystal potential for an atom denoted by index γ is given by the sum of the atomic potential of itself (γ atom) and those of the α atoms ($\alpha \neq \gamma$) surrounding the γ atom. Therefore, if we select an empty atom as the γ atom, it can be seen that the crystal potential for the empty atom is constructed from the atomic potentials of the real atoms surrounding the empty atom. The influence of the atomic potentials of the surrounding real atoms to the empty atom site increases with increasing distance r from the EL point. Since the atomic potential of the real atom is a Coulomb-like attractive potential, like the crystal potential for the empty atom, we can obtain a potential which is negative and decreases with increasing distance r . The

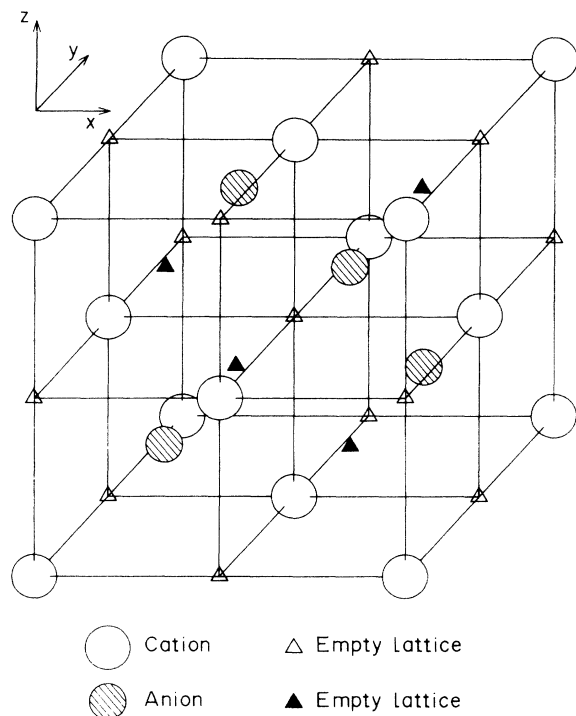


FIG. 1. Unit cell for zinc-blende-structure semiconductors used in the present paper. Open and hatched circles represent the cation and anion, respectively, and the structure constructed from those real atoms corresponds to a so-called "zinc-blende structure." Open and solid triangles represent empty lattices (EL's) defined in the present paper, and the positions of those EL's are defined, respectively, as the positions obtained by shifting the cation and anion by $a_0/2$ (a_0 is the lattice constant) along with the x axis. Note that this unit cell consists of eight small cubes, and each cube forms a bcc structure.

crystal potentials for the real atoms are obtained in the usual way which does not depend on whether the EL's are considered or not, as already mentioned in Sec. II A, the MT zero is given by the value obtained by averaging the crystal potentials over the whole volume except for the MT spheres region. Therefore, the resultant MT potentials measured from the MT zero become attractive for the real atoms and repulsive for the empty lattices. Circles and triangles indicated in Fig. 1 show the real atoms and empty lattices, respectively. Here it is very interesting to point out that the symmetry of the potential consisting of MT potentials on the real atoms and empty lattices coincides with that of the nonspherical potential, i.e., xyz , because the potential for an electron propagating in a crystal is attractive for the real atoms and repulsive for the empty lattices. Since the symmetry of xyz is the same as that of the sp^3 hybrids, for the study of the electronic structures of ZBS's by a method based on the MT approximation it would be important to consider the MT potentials on the EL sites in addition to those on the real atoms.

We have found that the MT potentials are attractive for real atoms and repulsive for EL's. This fact is easily understood if we focus our attention to a one-dimensional

atomic chain through the [100] direction of the ZBS's. The crystal potential for this one-dimensional atomic chain is shown schematically in Fig. 2. If we wish to study the electronic structure of this chain on the basis of the MT approximation, it is natural to adopt the value of $a_0/2$ as the MT radius; however, we are now considering ZBS's, so the MT radius must nearly be given by half the bond length $d_0/2$. Therefore, if we wish to study the electronic structure of ZBS's on the basis of the MT approximation, we must evaluate the crystal potential on the interstitial region between real atoms as correctly as possible. The potential on the interstitial region shown in Fig. 2 is just the crystal potential for the empty lattice. It is expected that the MT zero is nearly located on the energy position indicated by a broken line in Fig. 2, so that the MT potentials of ZBS's become an attractive form for real atoms and a repulsive one for EL's.

D. OPW band-structure calculations

The formulation of OPW band-structure calculations within the framework of the MT approximation based on the SCF atomic-structure calculations, which has already been given in Ref. 7, remains the same even if the EL-MT potentials are considered. The MT potentials are first principally calculated from Eqs. (1b), (2a), and (2b) by using the atomic data obtained from the SCF atomic-structure calculations, so the electronic structures of the ZBS's are calculated with no empirical parameters, except for how many OPW's are used in the practical calculations. In order to check how many OPW's are enough to obtain the converged result, first I carried out calculations using 89, 113, 181, and 259 OPW's. In these four calculations, the amplitudes G_{\max} of the maximum reciprocal-lattice vectors are given by $\sqrt{19}/2$, $\sqrt{5}$, $2\sqrt{2}$, and 3 in units of $4\pi/a_0$, respectively, so the corresponding kinetic energies G_{\max}^2 are, for example, evaluated as 97.0, 102.1, 163.3, and 183.8 eV for Si. As a result, I found that 113 OPW's are sufficient to obtain the converged results for all the valence bands and for the con-

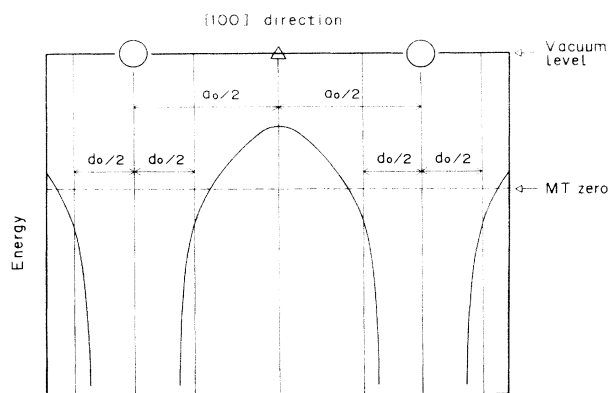


FIG. 2. Schematic diagram for the crystal potential of a one-dimensional atomic chain through a [100] direction of zinc-blende-structure semiconductors (ZBS's). The meaning of circles and a triangle is the same as in Fig. 1. The muffin-tin (MT) zero to be expected for the ZBS's is indicated by a broken line.

duction band up to about 10 eV from the conduction-band bottom; that is, we can say that in the electronic structure calculations for ZBS's based on the OPW method, the mathematical expansion of the wave function is complete enough if we use 113 OPW's and if we do not consider the structures of the higher conduction band distributed on an energy region larger than about 10 eV from the conduction-band bottom. This is the same number of OPW's adopted by Herman, Kortum, and Kuglin,¹⁵ who calculated the energy-band structure of silicon using the empirically adjusted OPW method. In the present paper, therefore, let us consider only how the crystal potentials of ZBS's should be represented within the framework of the MT approximation.

The densities of states (DOS's) are accumulated from 2048 numbers of the sampling points defined within the first Brillouin zone as the forms of histograms with an energy resolution of 0.25 eV. It is of course possible to calculate the DOS's in more detail if we do not consider the large CPU time required for those calculations.

III. RESULTS AND DISCUSSION

A. MT potentials

As an example, the MT potentials calculated for CdTe are shown in Fig. 3 along with the [111] and [100] directions. The calculated MT zero is -13.0 eV measured from the vacuum level, and the calculated MT radii are 2.5351 and 2.7674 a.u. for Cd and Te atoms, respectively, so those values are also equal to the MT radii of the EL-MT potentials originating from the shifts of cation and anion. For the EL, the spherical term $V_{\text{cry}}^{(s)}(r)$ of a crystal potential is constructed from the sum of the integrated values of the short-range-type functions $W(r_\alpha)$ and $\rho^{\text{at}}(r_\alpha)$ in the region between $R_\alpha - r$ and $R_\alpha + r$ apart from the Madelung term given by a constant value, be-

cause $V_c^{\text{at}}(r)$ and $\rho^{\text{at}}(r)$ in Eqs. (2a) and (2b) are zero for the empty atom. Therefore, if we consider a very small distance r measured from the EL point, the integrated value also becomes very small. Since the atomic potential and the atomic electron density for the empty atom are zero, the resultant crystal potential for the empty atom is given by zero (= vacuum level) in the very small value of r . This is the reason why the EL-MT potential forms a pointed structure in the vicinity of the EL point. It is noted that the Fourier components of the crystal potential are evaluated by the integral defined by Eq. (B6) in Ref. 7, so that the pointed structure in the vicinity of EL point of the EL-MT potential makes no significant contribution to the Fourier components of the crystal potential. Hereafter, we call the EL-MT potential the "bell potential" from its shape.

The energy value obtained by averaging the bell potentials, which is -9.08 eV measured from the vacuum level, is indicated by a broken line in Fig. 3. As already mentioned in the second paragraph in Sec. II A, if this value $V_{\text{MTZ}}^{(\text{Mod})}$ is used as a MT zero, instead of the MT zero $V_{\text{MTZ}}^{(\text{True})}$ obtained by averaging the crystal potentials over the whole volume except for the MT spheres region, it is expected that the results obtained by the ordinary calculational procedure will be improved.

B. Results for CdTe

First, the density of states (DOS's) obtained by using the ordinary calculations procedure, i.e., without the bell potentials, are shown in Figs. 4(a) and 4(b). The DOS's drawn in Figs. 4(a) and 4(b) have been obtained by using the $V_{\text{MTZ}}^{(\text{True})}$ and $V_{\text{MTZ}}^{(\text{Mod})}$, respectively, mentioned in Sec. III A as the MT zero. From the meaning that there is no energy gap in Fig. 4(a) but well-resolved gap in Fig. 4(b), we can see that, within the framework of the ordinary calculational procedure, results are fairly improved by varying the magnitude of the MT zero, and that this vari-

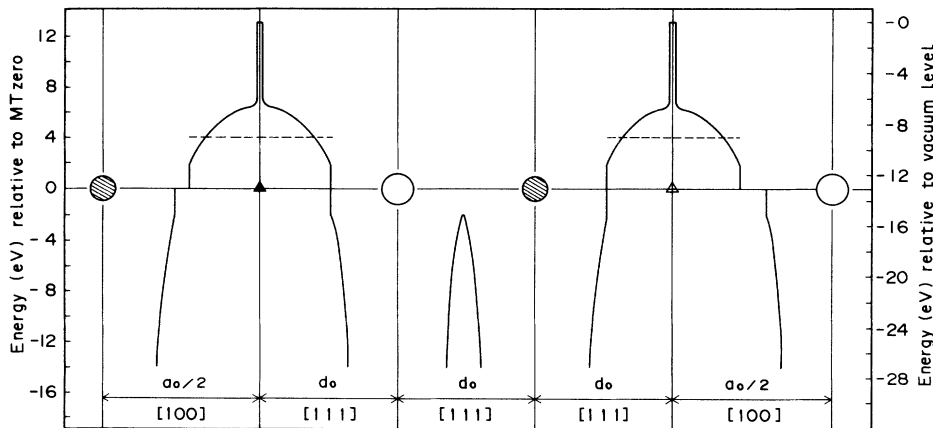


FIG. 3. Muffin-tin (MT) potentials on Cd, Te, and empty lattice (EL) sites of CdTe drawn through the [111] and [100] directions. In the present paper, the MT potentials on the EL's (EL-MT potentials) are referred to as bell potentials from those shapes. The meaning of the circles and triangles is the same as in Fig. 1. Note that the calculations of the MT potentials are carried out in first principles for not only the real atoms but also for the EL's. The energy value obtained by averaging the bell potentials is also indicated by a broken line.

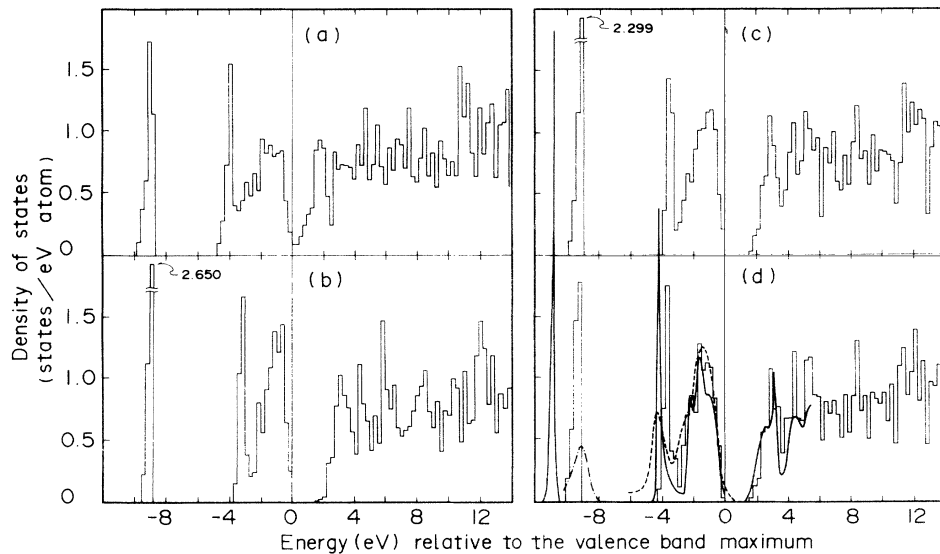


FIG. 4. The density of states (DOS's) of CdTe obtained from the different four calculational conditions. The bell potentials are not used in (a) and (b), and are used in (c) and (d). In (b), the value $V_{\text{MTZ}}^{(\text{Mod})}$ obtained by averaging the bell potentials has been used as a muffin-tin (MT) zero, instead of the MT zero $V_{\text{MTZ}}^{(\text{True})}$ obtained by averaging the crystal potentials over the whole volume except for the MT spheres region. In (a), (c), and (d), $V_{\text{MTZ}}^{(\text{True})}$ has been used as the MT zero. Moreover, in (d), the nonspherical potential defined by Eq. (5) has been introduced by adjusting the value of Z_{FNN}^* so as to fit the experimental value of a direct energy gap of CdTe. The comparison of the calculated DOS's with the others is made in (d), in which the DOS's calculated by Wei and Zunger (Ref. 10) on the basis of the linearized-augmented-plane-wave (LAPW) method and the photoemission spectrum observed by Eastman *et al.* (Ref. 17) are shown by solid and broken curves, respectively. Note that the spectrum shown by a one-dot broken curve around -9 eV in (d) is the DOS's that originated from the Te $5s$ level roughly estimated by Eastman *et al.*

ation would be closely related to the existing of the bell potentials.

Next, the DOS's calculated by introducing the bell potentials in addition to the MT potentials on real atoms are shown in Fig. 4(c), and furthermore those obtained by using not only the bell potential but also the nonspherical potential, which is adjusted by the value of Z_{FNN}^* so that the direct energy gap coincides with the experimental one of 1.59 eV at 4 K (Ref. 16), are shown in Fig. 4(d). Here it is noted that the results in Figs. 4(c) and 4(d) have been obtained by using the $V_{\text{MTZ}}^{(\text{True})}$ as the MT zero. By comparing the calculated DOS's drawn in Figs. 4(c) and 4(d), we find that (1) the width and shape of the upper valence band are almost the same; (2) the lower valence band indicating the sharpened shape is located in nearly the same energy region; (3) the energy gap estimated from the DOS's is exactly the same; and (4) the shape of the conduction band is very similar. The facts mentioned above explicitly indicate that in CdTe, the effect of the nonspherical potentials taken into account by Eq. (5) is not so large. Actually, the adjusted value for the Z_{FNN}^* was 2.34, so the resultant absolute value of the energy of the nonspherical potential on the midpoint of the bond was 3.33 eV. We will see in Sec. III C that the nonspherical potential defined by Eq. (5) makes a significant contribution to the electronic structure of Si.

Finally, let us compare the calculated DOS's with the experiment and other calculation. The DOS's calculated

using the LAPW method by Wei and Zunger¹⁰ and the photoemission spectrum observed by Eastman *et al.*¹⁷ are drawn by solid and broken curves, respectively, in Fig. 4(d). Here it is noted that Wei and Zunger used the same value of 2.53 a.u. for all the atoms as the MT radius, but I could not recognize the value they used for the MT zero because there is no description of the MT zero. Moreover, the DOS's calculated by Wei and Zunger have not been indicated by an absolute scale, so there results have been drawn in Fig. 4(d) in such a way that the amplitude of the upper valence band nearly coincides with that of mine. From the comparison of the present result with Wei and Zunger's and the experiment, we can see that (1) the width and shape of the calculated upper valence band are almost the same and that the experimental spectrum is fairly well predicted by both calculations; (2) the width and the shape of the conduction band distributed on the energy region up to about 3 eV from the conduction-band bottom are also nearly the same; but (3) for the lower valence band originating from a Te $5s$ level, there is a not negligible difference between the present result and Wei and Zunger's, and from a comparison with the experimental spectrum indicated by a one-dot broken curve; and (4) the present result predicts the energy position of states originating from the Te $5s$ level rather better than Wei and Zunger's result.

From the above discussion, it is concluded that in a CdTe, the effect of the nonspherical potential is not so

large, and that for the study of the electronic structure by the method based on the MT approximation it is essential to consider the bell potentials.

C. Results for Si

The dispersion relations obtained for several calculational conditions are shown in Fig. 5 along with the Δ axis. The results drawn in Figs. 5(a), 5(b), and 5(c), respectively, are the results calculated by using 0.0, 10.0, and 14.0 as the values of Z_{FNN}^* without the bell potentials, and those in Figs. 5(d) and 5(e) the results calculated by using 0.0 and 10.0 as the Z_{FNN}^* and including both the MT potentials for the real atoms and the bell potentials. In the present paper, I am interested in how the electronic structure of matter with small packing fractions should be treated by a method based on the MT approximation. Therefore, if we are not interested in the method but only in the electronic structures, we should calculate the electronic structures of matter by one method in some methods widely accepted. As already described in Sec. I, there are many methods to calculate the electronic structure of matters, and for the electronic structure calculations of zinc-blende-structure semiconductors (ZBS's)

with small packing fractions, it is well known that the empirical pseudopotential method (EPM) used by Cohen and Chelikowsky⁹ leads to excellent results not only for the valence band but for also the conduction band, because in the EPM, Fourier components of the pseudopotential are adjusted so as to fit the experiments. In the present paper, therefore, results calculated by using the EPM are used as a standard for the comparison of the present results with others when there are no experimental data. From the comparison of the present results with the result drawn in Fig. 5(f) which has been calculated by Cohen and Chelikowsky, we can see that the dispersion relation drawn in Fig. 5(e) well represents that of Si. In order to see how the energy eigenvalue is changed by the calculational condition, energies for irreducible representations Γ_{15} , Γ'_{25} , Γ , and X_{1c} are plotted in Fig. 6 as a function of Z_{FNN}^* for two cases: one is the case without the bell potentials, drawn in Fig. 6(a), and the other the case including all the potentials, shown in Fig. 6(b). I have already mentioned that the value of Z_{FNN}^* is decided in such a way that the calculated result coincides with the experiment or other calculations. If we approximately regard the indirect energy gap of Si as the difference of energies on the X_{1c} and Γ'_{25} , in the case without the bell

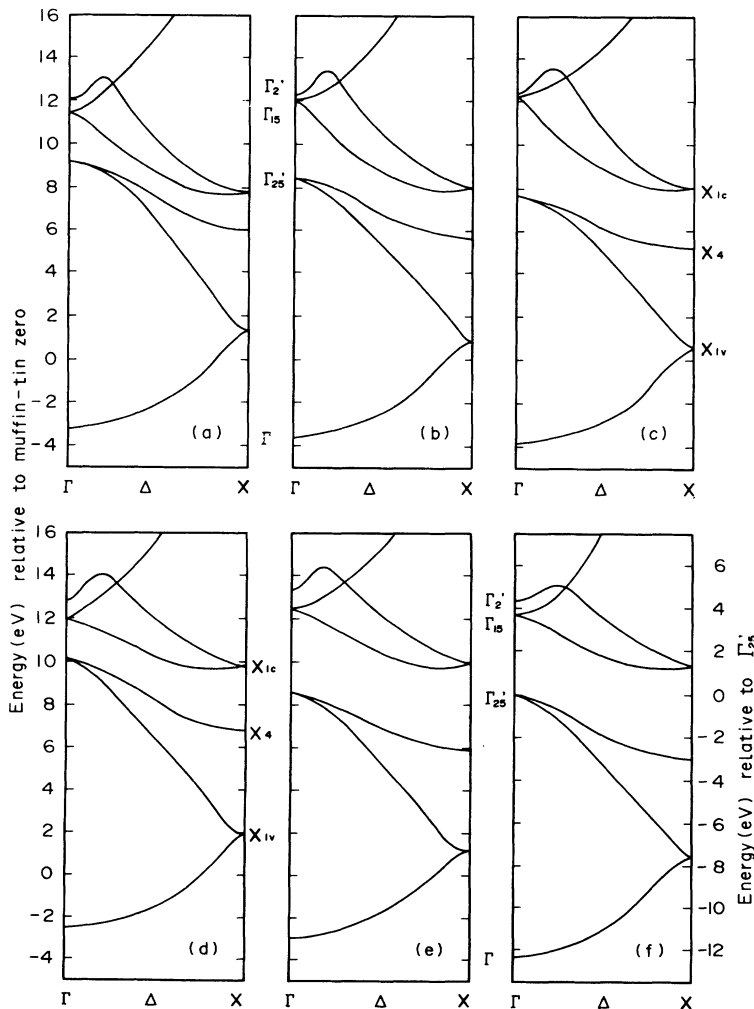


FIG. 5. Dispersion relations of Si calculated through the Δ axis. Results shown in (a), (b), and (c) have been obtained by using 0, 10.0, and 14.0 as the value of Z_{FNN}^* without bell potentials, and the results in (d) and (e) have been obtained by using 0 and 10.0 as the value of Z_{FNN}^* and including the MT potentials for both real atoms and bell potentials. For the comparison, the dispersion relation calculated by Cohen and Chelikowsky (Ref. 9) is shown in (f). Irreducible representations Γ , Γ'_{25} , Γ_{15} , Γ'_2 , X_{1c} , X_4 , and X_{1v} are also indicated.

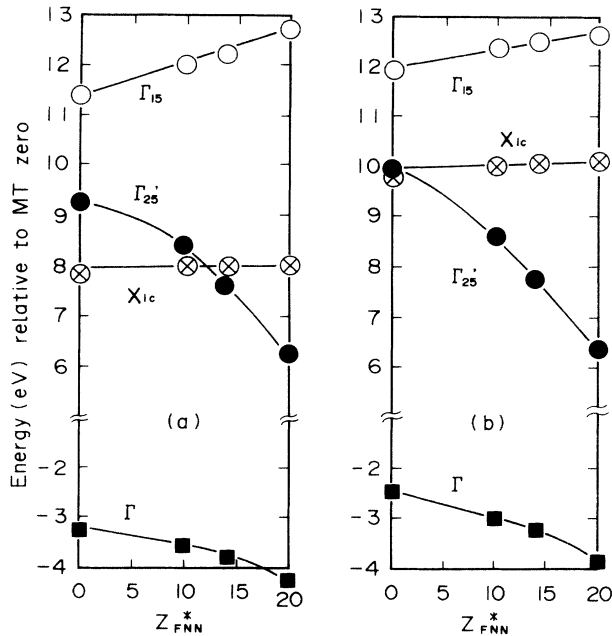


FIG. 6. Changes of the energy eigenvalues for Γ , Γ'_{25} , Γ'_{15} , and X_{1c} of Si due to the change of the value of Z^*_{FNN} characterizing the nonspherical potential defined by Eq. (5). Results in (a) have been obtained without the bell potentials, and those in (b) with the MT potentials for both real atoms and bell potentials. Note that the difference of the energy eigenvalues for X_{1c} and Γ'_{25} approximately gives an indirect energy gap for Si, whose experimental value is 1.1696 eV at 4 K (Ref. 18).

potentials we obtain 18 as the value of Z^*_{FNN} since the indirect gap of Si is known experimentally as 1.1696 eV at 4 K.¹⁸ Using this value, the width of the valence band and the direct energy gap on the Γ point are determined as 10.7 and 5.9 eV; however, there seems to be a considerable difference between these values and the values of 12.4 eV for the former and 3.7 eV for the latter, which have been deduced from the result of Cohen and Chelikowsky. Furthermore, it is noted that the adjusted value 18 for Z^*_{FNN} is larger than 14, which is the atomic number of Si. From the same analysis for the case including both MT potentials on real atoms and bell potentials, we obtain 10 as the value of the Z^*_{FNN} and obtain 11.6 eV as the width of the valence band and 3.8 eV as the direct energy gap on the Γ point. It is found that these values are in good agreement with the values of 12.4 and 3.7 eV of Cohen and Chelikowsky.

The DOS's obtained by using the value of 18 as the Z^*_{FNN} without bell potentials and those using 10 as the Z^*_{FNN} with bell potentials are shown in Figs. 7(a) and 7(b), respectively, together with the photoemission spectrum observed by Ley *et al.*¹⁹ and the DOS's calculated by Cohen and Chelikowsky,⁹ CC-DOS's, which are shown in Fig. 7(b) by broken and solid curves. By comparing the present results with the experiment and CC-DOS's, we can see that (1) the calculation including both the nonspherical and bell potentials well predicts the experimental fact, and (2) the agreement between the calcu-

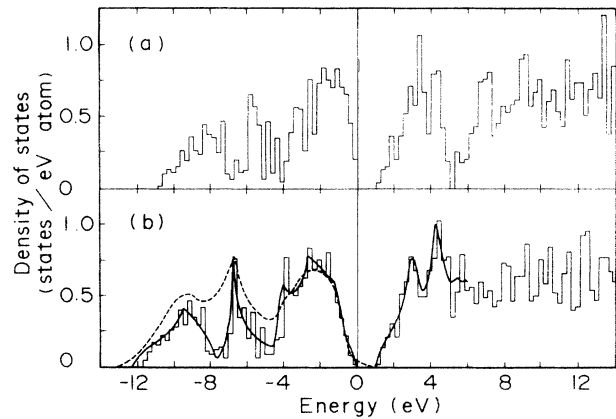


FIG. 7. The densities of states (DOS's) of Si obtained from the two different calculational conditions as follows: (a) The bell potentials have not been used, and a value of 18 has been adopted for Z^*_{FNN} . (b) The bell potentials have been used, and a value of 10 has been adopted for Z^*_{FNN} . The calculated DOS's are compared with the photoemission spectrum observed by Ley *et al.* (Ref. 19) and the DOS's calculated by Cohen and Chelikowsky (Ref. 9), which are shown in (b) by broken and solid curves, respectively. The energy is measured from the valence-band maximum.

lated DOS's shown in Fig. 7(b) and the CC-DOS's is excellent for not only the valence band but also the conduction band.

From the facts mentioned above, we can conclude that, in Si, the effect of the nonspherical potential is not negligibly small. For example, the absolute value of the energy of the nonspherical potential on a midpoint of the bond is 17.0 eV, which is about five times larger than that of CdTe. In order to explain the electronic structures by a method based on the MT approximation, it is crucial to consider not only the nonspherical potential but also the bell potential in addition to the MT potentials on the real atoms.

D. Overall result

By introducing the nonspherical potentials and the bell potentials into the OPW band-structure calculations based on the MT approximation, I have calculated the density of states (DOS's) for common semiconductors Si, Ge, GaAs, ZnSe, InSb, and CdTe. The calculated DOS's are shown in Figs. 8(a)–8(f) as shapes of a histogram together with the photoemission spectra observed by Ley *et al.*¹⁹ for Si and by Eastman *et al.*¹⁷ for the others. Furthermore, the DOS's for Si, Ge, GaAs, and ZnSe calculated by Cohen and Chelikowsky⁹ are also drawn by solid curves in Figs. 8(a), 8(b), 8(c), and 8(d). From a comparison of the calculated results with the results of Cohen and Chelikowsky, we can see that there are no significant differences between the present results and theirs. Moreover, the calculated results predict fairly well the photoemission spectra if the amplitude in the low-energy side of the valence band is overlooked.

In the present calculations, the values of 10.0, 9.14,

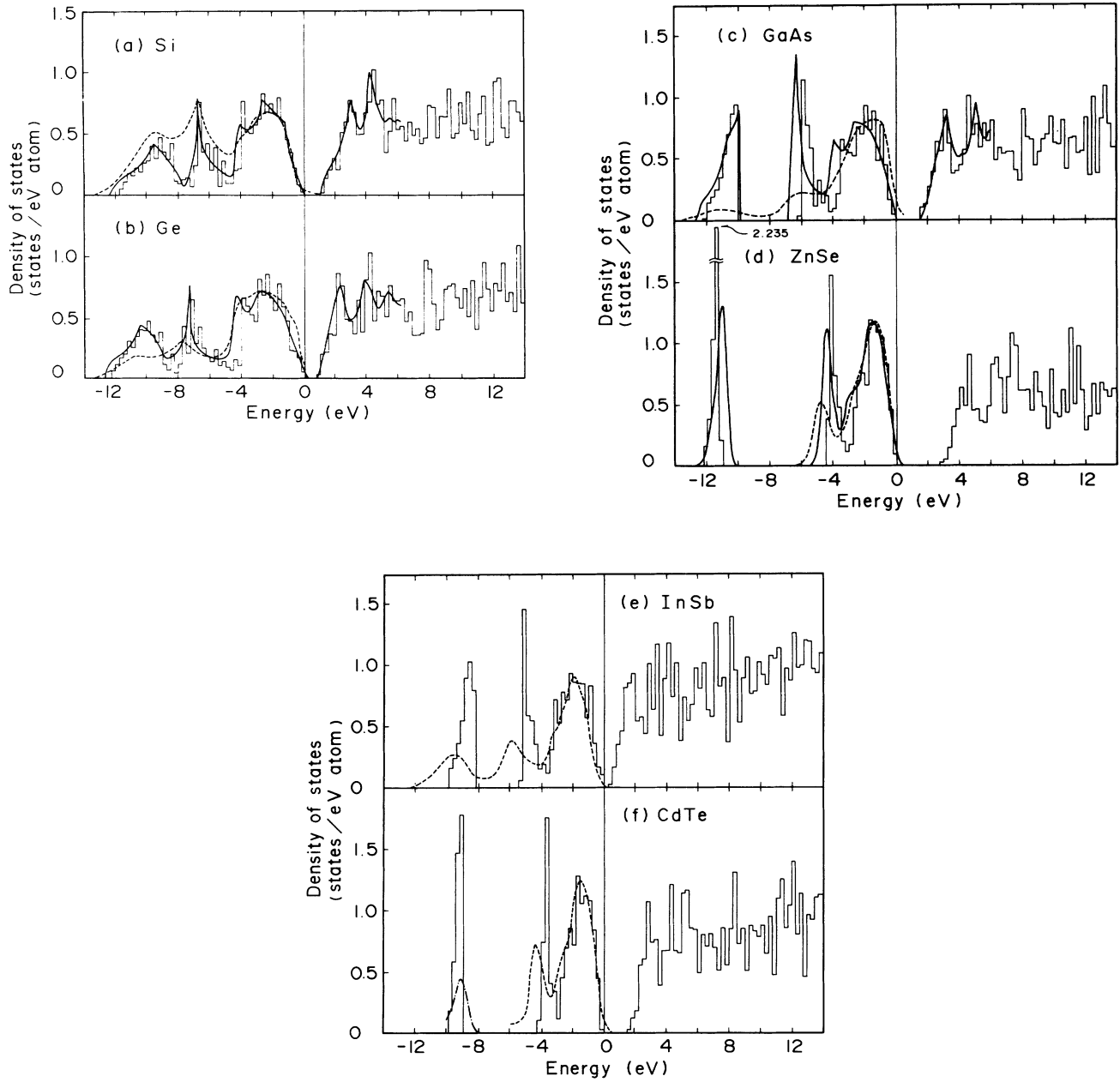


FIG. 8. Densities of states (DOS's) calculated as a shape of the histogram for Si (a), Ge (b), GaAs (c), ZnSe (d), InSb (e), and CdTe (f). For comparison, the DOS's for Si, Ge, GaAs, and ZnSe calculated by Cohen and Chelikowsky (Ref. 9) are indicated by solid curves in (a), (b), (c), and (d), and the photoemission spectra observed by Ley *et al.* (Ref. 19) for Si, and by Eastman *et al.* (Ref. 17) for others are drawn by broken curves. The energy is measured from the valence-band maximum.

8.92, 9.20, 1.30, and 2.34 have been used as those of Z_{FNN}^* 's for Si, Ge, GaAs, ZnSe, InSb, and CdTe. I can say that those values are always smaller than the atomic numbers of calculated semiconductors; however, I cannot present the physical meaning for the values of the Z_{FNN}^* 's used at the present time, because, as described in Sec. II B, Z_{FNN}^* is the constant value based on an assumption introduced in order to represent the nonspherical potential as an analytical form. I think that the physical consideration for Z_{FNN}^* should be given when the nonspheri-

cal potential is evaluated in a more accurate manner, e.g., numerical calculation.

IV. SUMMARY

The electronic structures of common semiconductors Si, Ge, GaAs, ZnSe, InSb, and CdTe have been calculated by using the orthogonalized-plane-wave (OPW) method within the framework of the muffin-tin (MT) approximation based on the self-consistent-field (SCF) atomic-

structure calculations. In the calculations, the effect of a nonspherical potential originating from the site symmetry of T_d has been considered, and Fourier components of the nonspherical potential have been added into those of the MT potential. Moreover, the MT potential on the empty lattice (EL) site, which has been called the bell potential because of its shape, has been calculated in first principles, and it has been shown that the symmetry of the potential consisting of MT potentials on real atoms and EL's coincides with that of the nonspherical potential reflecting the nature of sp^3 hybrids. It has been found that the present calculation including both nonspherical

and bell potentials predicts fairly well the experimental fact, and we point out that for a study of the electronic structures of semiconductors based on the MT approximation it is essential to consider not only the nonspherical potential but also the bell potential in addition to the MT potentials on the real atoms.

ACKNOWLEDGMENT

The author would like to thank Professor W. A. Harrison, Stanford University, for his valuable comments.

-
- ¹B. Alder, S. Fernbach, and M. Rotenberg, *Method in Computational Physics, Vol. 8: Energy Bands of Solids* (Academic, New York, 1968).
- ²A. A. Katsnelson, V. S. Stepanyuk, A. I. Szasz, and O. V. Farberovich, *Computational Methods in Condensed Matter: Electronic Structure* (American Institute of Physics, New York, 1992).
- ³M. Kitamura and S. Muramatsu, *Phys. Rev. B* **41**, 1158 (1990).
- ⁴M. Kitamura and S. Muramatsu, *Phys. Rev. B* **42**, 1417 (1990).
- ⁵M. Kitamura and W. A. Harrison, *Phys. Rev. B* **44**, 7941 (1991).
- ⁶M. Kitamura, S. Muramatsu, and W. A. Harrison, *Phys. Rev. B* **46**, 1351 (1992).
- ⁷M. Kitamura, *Phys. Rev. B* **49**, 1564 (1994).
- ⁸W. A. Harrison, *Electronic Structure and the Properties of Solids* (Freeman, New York, 1980) (reprinted by Dover, New York, 1988).
- ⁹M. L. Cohen and J. R. Chelikowsky, in *Handbook on Semiconductors*, edited by W. Paul (North-Holland, Amsterdam, 1982), Vol. 1.
- ¹⁰S.-H. Wei and A. Zunger, *Phys. Rev. B* **35**, 2340 (1987).
- ¹¹M. Kitamura, S. Muramatsu, and C. Sugiura, *Phys. Status Solidi B* **142**, 191 (1987).
- ¹²M. Kitamura, S. Muramatsu, and C. Sugiura, *Phys. Rev. B* **37**, 6486 (1988).
- ¹³P. M. Scop, *Phys. Rev.* **139**, A934 (1965).
- ¹⁴P. Eckelt, O. Madelung, and J. Treusch, *Phys. Rev. Lett.* **18**, 656 (1967).
- ¹⁵F. Herman, R. L. Kortum, and C. D. Kuglin, *Int. J. Quantum Chem.* **1S**, 533 (1967).
- ¹⁶H. Tamura and T. Masumi, *Solid State Commun.* **12**, 1183 (1973).
- ¹⁷D. E. Eastman, W. D. Grobman, J. L. Freeouf, and M. Erbudak, *Phys. Rev. B* **9**, 3473 (1974).
- ¹⁸J. C. Hensel, T. G. Phillips, and G. A. Thomas, in *Solid State Physics*, edited by F. Seitz *et al.* (Academic, New York, 1977), Vol. 32.
- ¹⁹L. Ley, R. A. Pollak, F. R. McFeely, S. P. Kowalczyk, and D. A. Shirley, *Phys. Rev. B* **9**, 600 (1974).